Probabilistic Analysis of Monitoring Systems for Detecting Subsurface Contaminant Plumes

by A.W. Warrick[a], M.H. Young[a,b], and P.J. Wierenga[a]

Abstract

We study the probabilities that monitoring systems will be capable of detecting subsurface contaminant plumes. The analysis is an extension of previous research which focused on detection of ore bodies and contaminant releases to the subsurface using probabilistic models; the previous research assumed that releases to the subsurface are elliptical in shape, and that detections are absolute when a monitoring point intercepts a release. New features are introduced into the analytical framework that include irregular, rather than regular, sampling arrays, as well as nonuniform probabilities of a release occurring at a particular location of the site. These features allow the user to optimize the location of sampling devices based on site knowledge, by concentrating monitoring locations where a release is believed more likely. The stratified Monte Carlo approach used in this paper is tested on a number of cases with uniform and nonuniform sampler distribution and release probabilities. The results provide statistical probabilities that one is capable of finding releases of different sizes with a system of monitoring points.

Introduction

Monitoring hydrologic conditions below waste disposal sites is desirable to minimize future environmental damage during operational and post-operational time periods. However, methods for evaluating monitoring system efficiency can be difficult to apply without ready access to objective analytical techniques. Designers and regulators must rely solely on training and experience to guide them toward a decision on acceptability. Given the range of experiences from person to person, subjective judgements could lead to different decisions about the same monitoring strategy.

Analytical tools that provide more objective analyses could assist the designers and regulators in their efforts to license and permit disposal facilities from operational through post-operational periods. The tools could be used to study what happens to a monitoring system if a monitoring point is removed from service (e.g., when a sensor fails), and whether it is financially worth the cost of adding a new monitoring point. Moreover, to minimize cost and improve the ability of the monitoring system to detect releases to the subsurface, it is important to optimize the number and placement of monitoring devices. Because contaminants may leak in some spots and not in others, monitoring systems need to be designed so that the likelihood of intercepting a contaminant plume is greatest for the number of devices available. Our research focuses on objectively evaluating monitoring systems installed in the vadose zone. This is analogous to detecting mineral deposits in geologic media (Gilbert 1987; Freeze et al. 1992; Keller 1996). In their studies, the latter authors also considered definitions of reliability. Similar studies were done by Drew (1967, 1979), who discussed pattern gridding for locating petroleum reserves in the United States. He considered optimum spacing of exploration boreholes, search theory, and detection probability.

Zirschky and Gilbert (1984) and Gilbert (1987) presented nomographs related to the probability of intercepting a randomly located elliptical release given a rectangular or triangular sampling pattern. They assumed that only a very small proportion of the area was sampled and that the detection is clearly "yes" or "no." Calculations were performed with the Elipgrid program (Singer 1972). The plume used in Gilbert's work was elliptical in cross section; detection was assumed if a sampling grid point intercepted the ellipse. Nomographs relate, for example, the probability that the plume will be missed by the sampling points (called consumer risk) given an ellipse radius. the ratio of the semi-major and minor axes, the sampler spacing, and the sampling pattern. The probability of a hit was plotted as a function of the ratio of the sampler spacing to the release radius, with one curve for each drilling pattern and ellipse eccentricity. Davidson (1995a, 1995b) developed and tested a user-friendly version of Elipgrid called Elipgrid-PC. With this program, one can calculate, for a rectangular or triangular sampling pattern, the probability of at least one hit assuming an ellipsoidal plume of given size and orientation. Other options allow the user to solve for the grid size required to find a plume of a given size and shape at a given probability, or for the radius of the smallest release likely to be detected given the grid size and probability of a hit.

Monitoring network design also has been used to optimize the placement of monitoring points for detection monitoring at disposal sites. These points would be a component of a monitoring plan most likely implemented under U.S. EPA's RCRA program, where ground water impacts from the disposal site have not occurred and potential future impacts are sought to be minimized. Integer programming models have been used (for example, Loaiciga 1989 and Meyer et al. 1994) to balance out competing objectives of the monitoring system, such as minimizing the number of wells, maximizing the detection of contaminant plumes, and minimizing costs. These models can be incorporated into ground water flow and solute transport models of various complexities. A goal of the inte-

[a]Department of Soil, Water and Environmental Science, The University of Arizona, Tucson, AZ 85721.

[b]School of Civil and Environmental Engineering, Georgia Institute of Technology, Atlanta, GA 30332.

Received September 1997, accepted February 1998.

ger programming approach is to minimize an objective function that calculates the success (or failure) of the monitoring system to detect a plume subject to a number of competing objectives, several of which were listed previously. This approach can be made more all-encompassing by including Bayesian updating of parameter values based on prior knowledge of site-specific characteristics (Freeze et al. 1990; Small 1997). Bayesian updating reduces parameter uncertainty, and thus risks associated with making decisions about the number and locations of monitoring points and sampling frequency. These two approaches (integer programming and Bayesian updating) were shown to yield optimized monitoring locations for systems presented in their examples.

However, the cost of using these integer programming and Bayesian updating approaches is manifested by a need for more complicated model development and data needs. For many ground water or soil contamination problems, this level of complexity may not be warranted or possible. For those cases where a regulator, consultant, or researcher seeks to gain insight into monitoring issues, the simpler approach described herein may be more useful. Therefore, the objective of this study is to extend the work of Gilbert (1987) and Davidson (1995b). We calculate the probability of a randomly placed elliptical plume intersecting at least one of a number of fixed location samples.

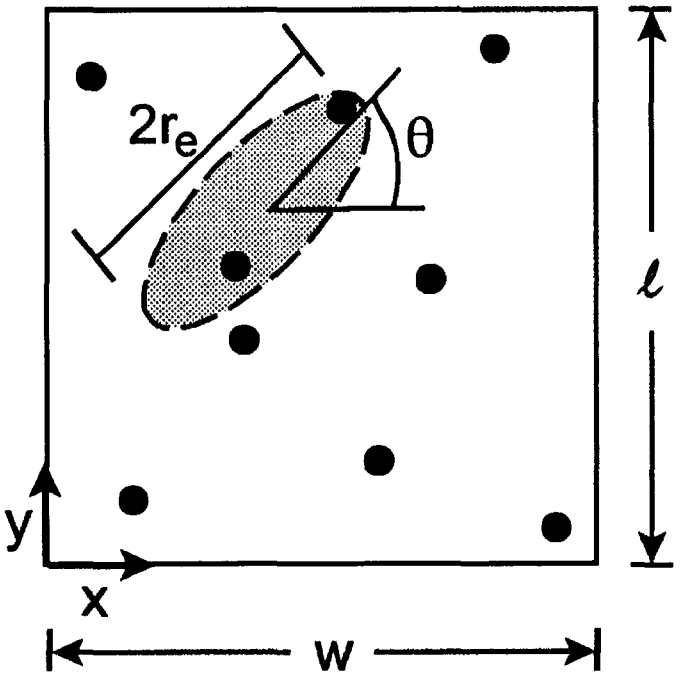

Figure 1. A rectangular field of width w and length ℓ. The dots denote sampler locations and a release is shown as the shaded ellipse with a semi-major axis of r_e and orientation angle θ.

Theoretical

Field and Release Probability Function px(x,y)

A rectangular field is considered (although in principle, any shape can be taken). In Figure 1, the field is taken of width w and length 1. An array of n sampling positions are located at coordinates (x_1,y_1), (x_2,y_2),...(x_n,y_n). Normally, all samplers would be within the field boundaries, although they could exist to the outside.

Within the field, the probability of a release $p_s(x,y)$ is defined with normalized integral of 1, i.e., the integral of $p_s(x,y)$ over the field is

$$\int_0^{\ell}\int_0^{w} p_s(x,y)dxdy = 1 \qquad (1)$$

The simplest case is when there is an equal probability of a release occurring anywhere in the field. This uniform probability function is simply a constant, $p_s(x,y) = (w\ \ell)^{-1}$. However, if prior knowledge suggests that release is more likely to occur in one part of the field than another, this can be reflected in choice of $p_s(x,y)$. For example, a higher probability may be assigned to the area corresponding to an original burial trench or along a hauling path.

Figure 2 shows two areal probability functions over a square field. On the left is a uniform distribution (with equal probability of a release anywhere in the field). This is the case considered implicitly by Gilbert (1987) and Davidson (1995a, 1995b). Also shown is a binormal release probability with the maximum probability in the center (i.e., along x = 0.5). The standard deviation is much smaller in the x-direction ($\sigma_x = 0.1$) than in the y-direction ($\sigma_y = 1$), where the values for σ_x and σ_y are normalized according to the field dimensions. The probability drops off rapidly from the center in the x-direction and only gradually in the y-direction. Other probability distributions could be chosen, including empirical as well as specified continuous functions.

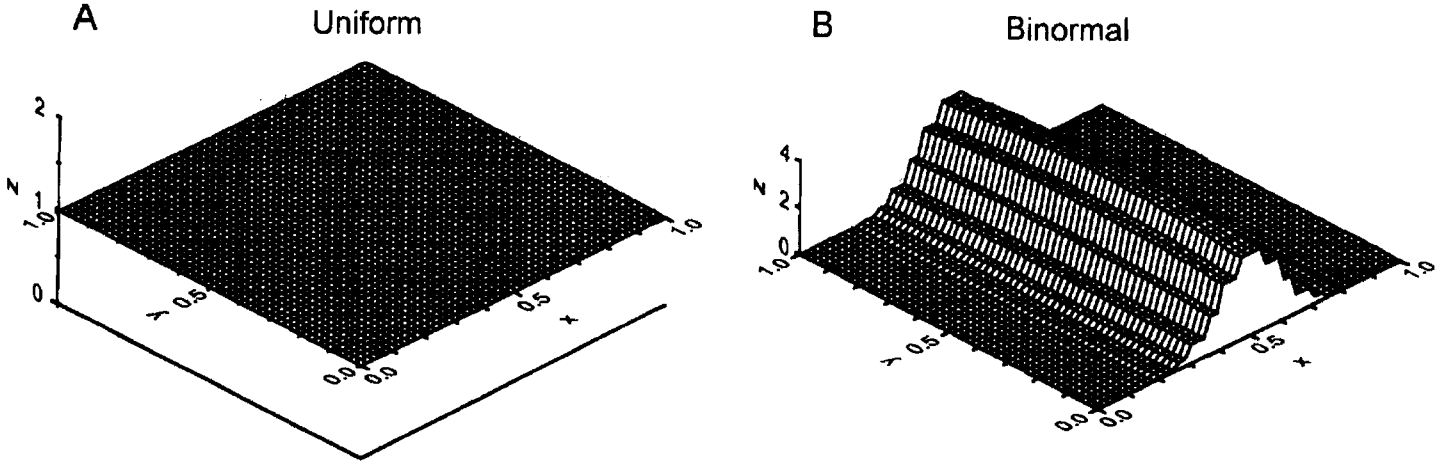

Figure 2. A uniform and binormal probability distribution. The binormal distribution is centered at x = 0.5 and y = 0.5 with standard deviations of $\sigma_x = 0.1$ and $\sigma_y = 1$.

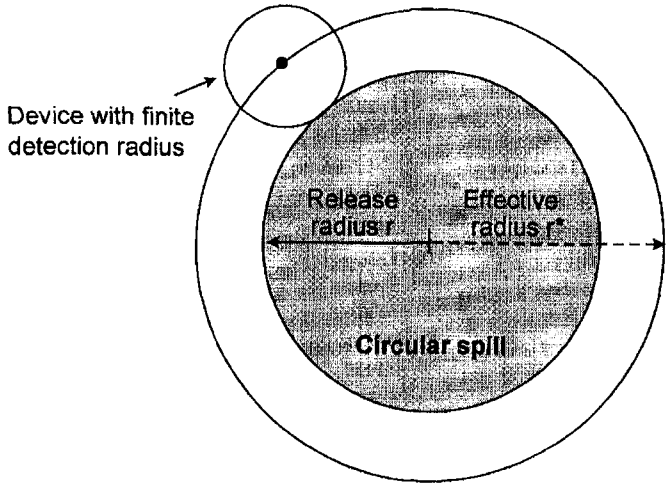

Figure 3. A circular release and a device with a finite detection radius to the outside. The effective radius r* is the sum of r and the detection radius of the device.

Sampling Device with a Finite Detection Radius

An assumption of the analyses by Gilbert (1987) and Davidson (1995a, 1995b) is that each sampler is sensitive only at a point and detection occurs when that point is included within the release ellipse. This is addressed briefly by Keller (1996). For a finite detection radius and a circular release, the result is the same as if the radius of the release r is enlarged by the sampling radius of this device. This is shown as r* in Figure 3. The sampler is ineffective only when it is outside of r*. For an elliptical release the same principle applies.

Parameterization of an Elliptical Plume

A contaminant plume is assumed to be elliptical (as in Gilbert [1987] and Davidson [1995a, 1995b]). The ellipse is characterized by the major semi-axis r_e, an aspect a_e defined as the ratio of the minor to major axes and, finally, an orientation angle θ chosen between the major axis of the ellipse and the horizontal. Such an ellipse is depicted in Figure 1. Whether the ellipse intersects any sampling points obviously will depend on sampler locations, where the ellipse is placed, and the radius, aspect, and orientation of the ellipse.

For an ellipse centered at (x_e,y_e), it becomes necessary to know whether a sampling point (x_s,y_s) is intersected, i.e., falls within the boundary of the ellipse. With this in mind, it is convenient to define a coordinate system (x',y'), centered on the ellipse with x' directed along the major axis (Figure 4a). The sample point in terms of the new coordinate system is (x_s',y_s') with (Davidson 1995b, esp. p. 14):

$$x_s' = (x_s - x_e)\cos\theta + (y_s - y_e)\sin\theta \tag{2}$$

and

$$y_s' = (y_s - y_e)\cos\theta - (x_s - x_e)\sin\theta \tag{3}$$

The equation of the ellipse can be written in the form

$$(x')^2 + \frac{(y')^2}{a_e^2} = r_e^2 \tag{4}$$

with r_e and a_e defined as before (of course, for a circle, a_e is unity and the orientation angle can be taken as zero). The point (x_s',y_s') will fall inside or on the boundary of the ellipse provided

$$(x_s')^2 + \frac{(y_s')^2}{a_e^2} \le r_e^2 \tag{5}$$

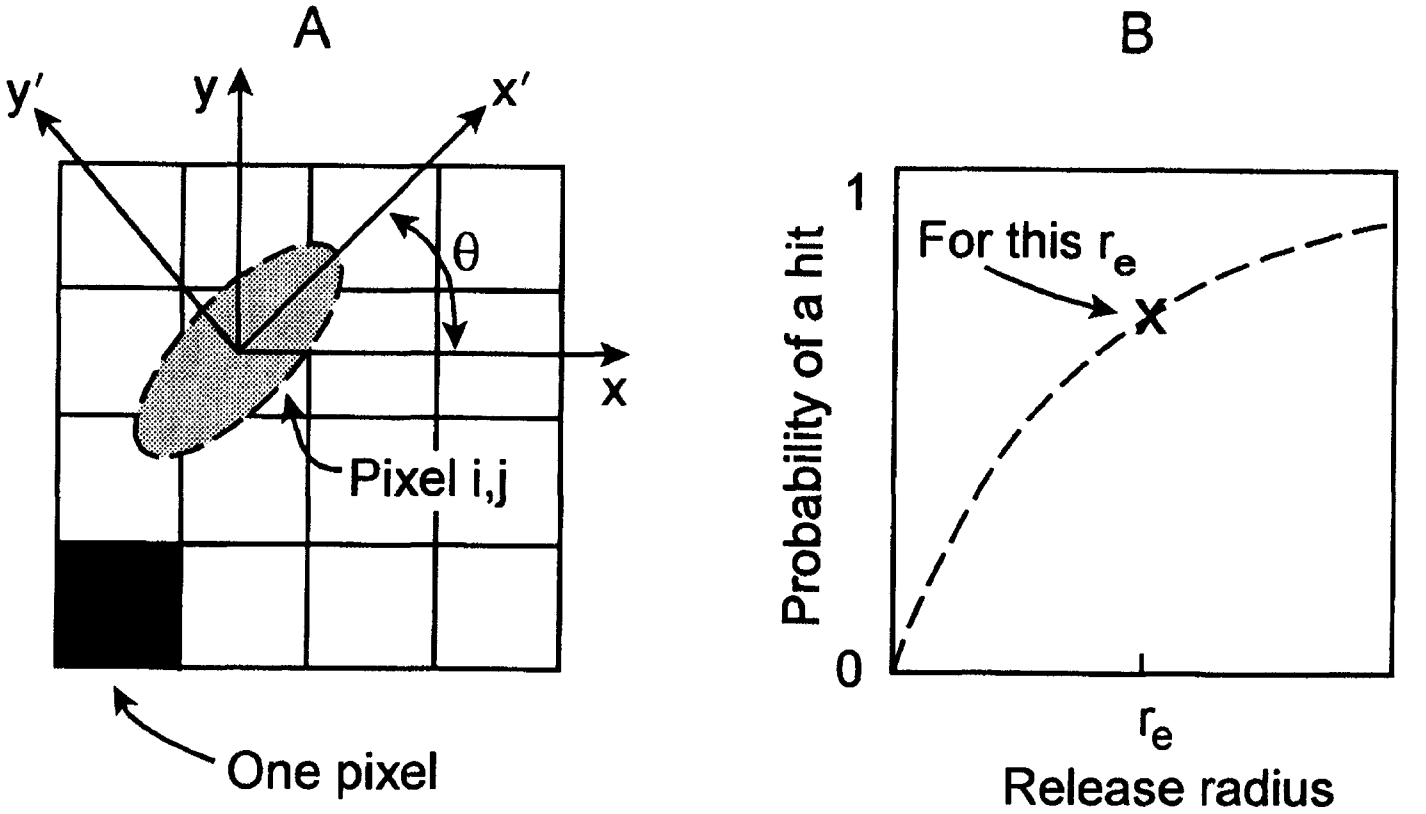

Figure 4. Coordinates oriented with the release ellipse (x', y') centered over pixel i,j (a). An ellipse of radius of r_e will result in one point on the curve showing probability of a hit (b). The release radius r_e is defined as the length of the major semi-axis of the ellipse.

Monte Carlo Strategies

A Monte Carlo simulation is a method useful for many types of problems. In this case, the method may be considered as a numerical sampling technique which is repeated a large number of times, in order to evaluate the probability of whether a sampling point intercepts an elliptical release. Although Elipgrid and the Elipgrid-PC programs originally used geometric relationships to determine whether a fixed-grid system intercepted a randomly placed elliptical plume, a later version (Davidson 1995b) used a Monte Carlo technique for the same problem.

For a simplified Monte Carlo simulation (Hammersley and Handscomb 1964), a random point (x_1,y_1) is chosen on the field of interest according to the probability distribution $p_s(x,y)$ describing the release. If the release probability distribution is totally random (Figure 2a), then (x_1,y_1) is chosen from a uniform distribution. If the distribution along x and y each satisfy a normal (or some other) distribution (Figure 2b), then (x_1,y_1) would be chosen following that distribution. Once the random point is chosen, then Equation 5 is used to determine whether any of the existing sampling points fall under the ellipse. If so, a value for a hit $h_1 = 1$ is assigned; otherwise the ellipse does not fall over any of the points and $h_1 = 0$. Additional points (x_2,y_2), (x_3,y_3),...(x_n,y_n) are chosen and $h_2,h_3,\ldots h_n$ are found. The probability of a hit for randomly chosen release is approximated by averaging the n values of h_i

$$P \approx \frac{1}{n}\sum_{i=1}^{n} h_i \qquad (6)$$

As n becomes large, P converges to the true probability.

Although this Monte Carlo scheme is simple in principle, generally, stratified methods are more efficient (Hammersley and Handscomb 1964). With this in mind, we choose a stratified scheme by dividing the field into n = (nx)(ny) pixels arranged in nx columns and ny rows (Figure 4a). An individual pixel i,j with center at (x_i,y_j) is shown. An ellipse is centered over the center of each pixel and the hit value $h_{ij} = 0$ or 1 determined as above. The probability of a randomly placed ellipse must take into account the spatial dependence of the release probability $p_s(x,y)$ and P becomes

$$P \approx \sum_{i=1}^{nx}\sum_{j=1}^{ny} h_{ij} p_s(x_i,y_j)\,\delta A_{ij} \qquad (7)$$

where δA_{ij} is the area of pixel i,j. As nx, ny become large, P approaches the true probability P given by

$$P = \int_0^{\ell}\int_0^{w} h(x,y)\, p_s(x,y)\, dxdy \qquad (8)$$

The function h(x,y) depends on sampler locations and the radius, orientation, and aspect of the release; the function $p_s(x,y)$ depends on the release probability distribution.

If results are of interest for more than one radius of an ellipse, the Monte Carlo scheme can be repeated to define the probability as a function of radius of release (Figure 4b). Although radius is an obvious variable for plotting probability of a hit, other variables could be used, such as sampling density, aspect of ellipse, etc.

Numerical Examples

A program "detect.for" was written to carry out the stratified Monte Carlo scheme just described. Normal probability functions needed for defining $p_s(x,y)$ were from Abramowitz and Stegun (1964, esp. Equation 26.2.27). Sampler locations are read by a data file and probabilities of at least a single hit are calculated for an array of r values. All of the following examples were run with 10,000 pixels.

Example: Uniform Sampler Distribution and a Circular Release

A uniform 4×4 sampling pattern over a square field is considered first. The positions are shown in Figure 5 as well as contours showing the distribution of distances away from the sampling point. The maximum distance d_{max} away from the samplers occurs at internal points equidistant from four sampling points and at corresponding points on the boundary. For the square field, each point is centered in an equally sized pixel and d_{max} is

$$d_{max} = \frac{1}{2^{0.5}nx} = \frac{1}{2^{0.5}ny} = 0.177 \qquad (9)$$

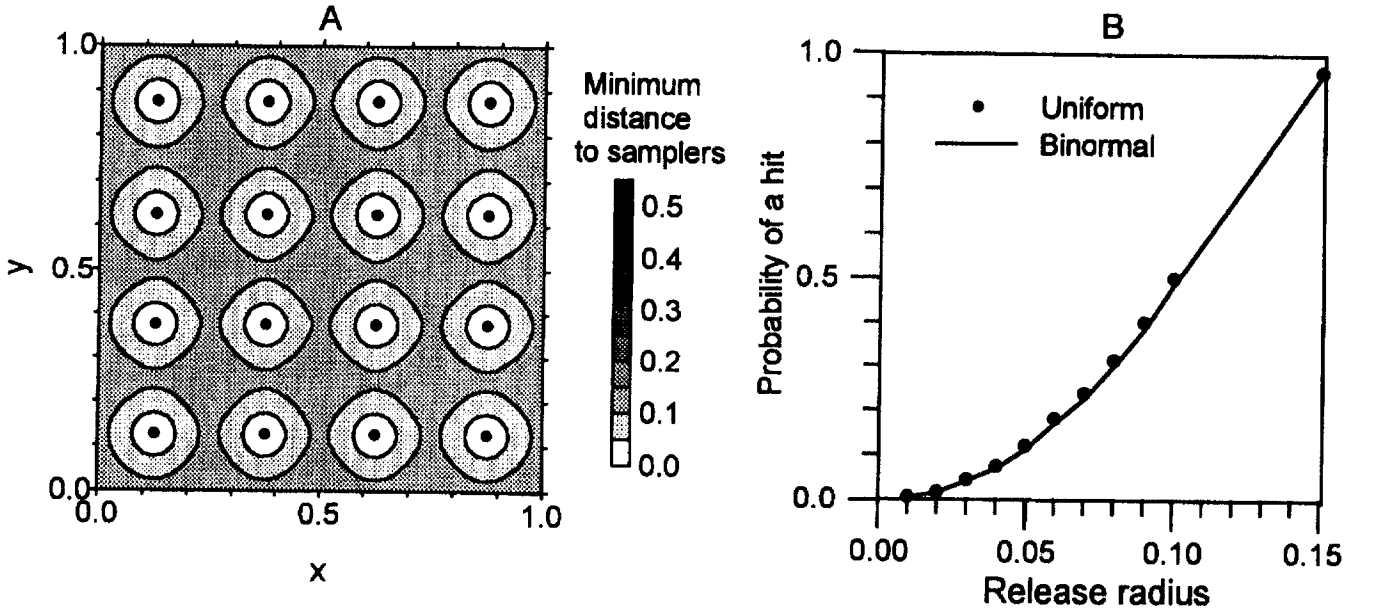

Figure 5. Uniform array of 16 detectors in a square field (a) and probabilities of a hit for circular releases with a uniform and binormal release probability (b).

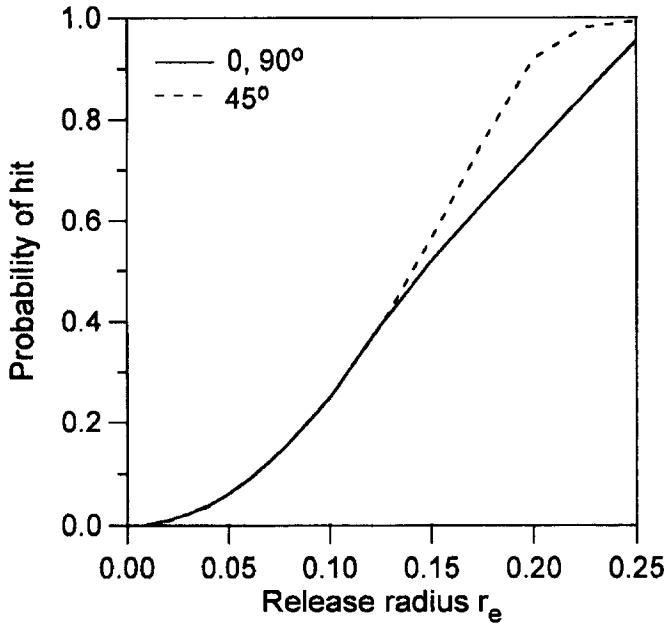

Figure 6. Probability of a hit for a release ellipse of r_e with orientation angles of θ = 0, 45, and 90 degrees. The sampling grid is as in Figure 5a and the release probability is uniform.

The resulting probabilities of at least a single hit are shown in Figure 5b for a uniform detector spacing and uniform release probability density function $p_s(x,y) = (w\ell)^{-1}$ (note length and widths of field are $\ell = 1$ and $w = 1$). For a tiny release radius, the probability of a hit is nearly zero. As the release radius increases, the probability value increases until it is impossible to miss with $r = d_{max} = 0.177$. Also, it is easy to show that when r is less than or equal to 0.5 Δx, no more than one sampling point can be intersected and the probability of this occurring is the fraction of the area covered by one circle overlying each sampling point, i.e., P is

$$P = \frac{\pi r^2}{\Delta x^2}, \quad 2r \le \Delta x = \Delta y \tag{10}$$

This result provides an analytical expression for checking some of the Monte Carlo results. For example, at a release radius r = 0.5 Δx = 0.125, the theoretical result is $P = \pi/4 = 0.785$, which can be compared to the plot.

Changing to the binormal release probability function given by Figure 2b does little to change the results for the uniform distribution of sampling points. This is illustrated by the solid line in Figure 5b which falls nearly on top of the results calculated for the uniform probability distribution.

Elliptical Release Example with a Square Sampling Pattern

The aforementioned probability calculations are repeated for ellipses where the ratio of the minor to major semi-axes is 0.5 (i.e., aspect = 0.5). For ellipses with major-semi axes oriented at θ = 0 and θ = 45 degrees, the results are shown in Figure 6 for a uniform distribution (this case is also included in Elipgrid, Davidson 1995a). The probability for small radii are independent of the direction, as the "area of interception" for each ellipse is exactly the same. However, the probability is higher for the 45 degree orientation as the radius becomes larger than about 0.12. As r becomes still larger, both results converge toward a probability of 1. For an orientation of θ = 90 degrees, the results are exactly the same as for 0 degrees for a square sampling pattern. Results were all calculated for the binormal probability distribution of Figure 2b, but are not shown as they are essentially the same as for the uniform $p_s(x,y)$ distribution.

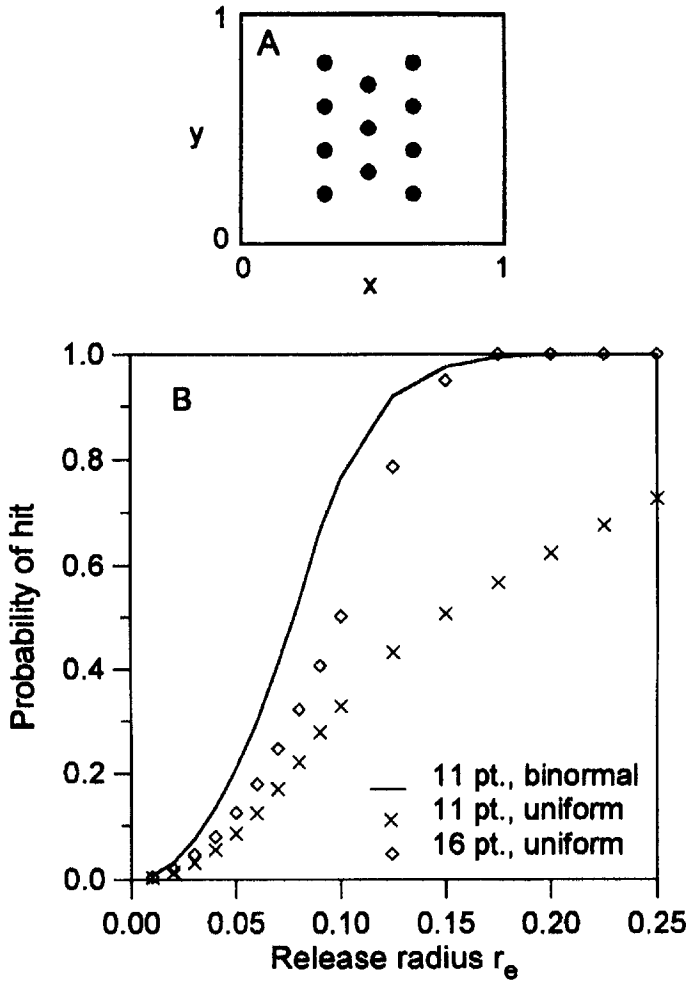

Figure 7. Eleven point sampler grid with three points along x = 0.5 (a) and probabilities of a single hit for both the binormal and uniform release probabilities (b). (The results for 16 samplers and a uniform release probability are repeated from Figure 5b.)

Circular Release Example with Concentration of Samplers in Zone of Higher Release Probability

In this case, an 11-point sampling pattern is chosen by first eliminating the samplers along x = 0.125 and x = 0.875 of Figure 5a. Three points are then added along x = 0.5 to the remaining eight points, as shown in Figure 7a. The probabilities of a single hit are calculated as a function of r for uniform release probability and given in Figure 7b. The result for the 16-sampler example is repeated for a direct comparison. The 16 samplers, of course, lead to higher probabilities of a single hit. The difference is especially striking as r becomes large (0.1 to 0.25) with the large difference due to the fact that no samplers are present in large regions to the left and right in the field. However, a different result is found if the release is more likely to occur along x = 0.5, in particular, with the release probability $p_s(x,y)$ defined as the binormal function of Figure 2b. In this case, with the 11-point sampler pattern, the probability of a single hit is considerably higher for smaller releases. For large r approaching 0.15 or so, both the 11-point pattern and the 16-point pattern are close to P = 1.

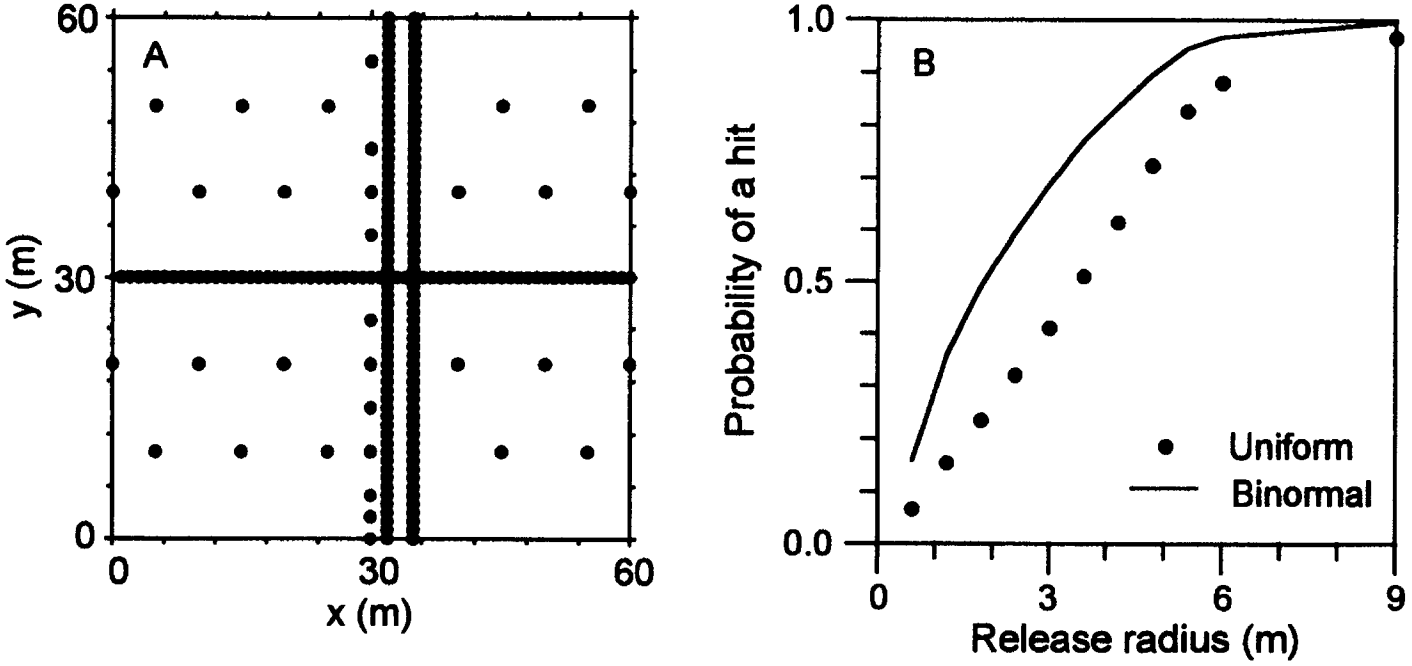

Figure 8. A dense 224-sampler array (a) and probabilities determined for the uniform and binormal release probabilities of Figure 2 (b).

Dense and Irregular Sampling Point Array

In a final example, 224 irregular samplers are considered on a 50 m × 50 m area. This represents an array of samplers in existence as part of a field monitoring study at the Maricopa Agricultural Center in Arizona (Young et al. 1996). The location of the samplers are shown as Figure 8a. Included are samplers only 1 m apart on three continuous transects—two in the y-direction and one in the x-direction. These represent subsurface horizontal tubes used for neutron thermalization determinations of soil water. An additional less intense transect of greater spacing is shown in the y-direction, as well as four additional but sparse transects in the x-direction. This sampling array leads to probabilities of hits shown in Figure 8b for uniform and binormal release probabilities. In this case, for small release radii, the probability of a hit is much larger for the binormal than for the uniform release probabilities. For example, compare $P \approx 0.4$ to $P < 0.2$ at a release radius of 1 m for the binormal and uniform cases, respectively. This reflects the higher probability of a release occurring along the center of the field for the binormal case, which coincides with the greater density of samplers. Eventually, for the large release radii (cf., r = 6 m or larger), the probability of a hit for both cases is about the same and close to unity. In this case, the release radius is approaching the maximum distance of any point of the field to an adjacent sampler.

Sources of Uncertainty in Analytical Approach

We have identified three possible sources of uncertainty in the analytical approach presented here, which are from (1) model development used to predict contaminant plume locations and size (including parameter and boundary condition uncertainties); (2) fitting of the release probability map to the predicted contaminant plume; and (3) the resolution (e.g., number of pixels) used in the search algorithm. For the purposes of this manuscript, we have not discussed model errors and uncertainties; though we believe that the uncertainties can be incorporated into the probability location map, sized either conservatively large or small depending on the application.

Uncertainties from fitting the probability location map to the predicted plume can be significant. Though not presented in this manuscript, probability maps can be generated for multiple contaminant plumes predicted for the same flow field. The maps can overlap one another or be placed in disparate areas. Normalizing is performed by summing values of $p_s(x,y)_i$ (from Equation 1) for all releases, where i varies from one to the number of probability location maps chosen by the user. The Monte Carlo algorithm then proceeds as described before. In this way, multiple, or odd-shaped, predicted plumes can be more closely approximated than if a single location map were used, reducing uncertainty from the fitting.

Uncertainties from pixel resolution were studied by taking the example presented in Figure 7 (11 point, binormal), using the binormal probability distribution from Figure 2b, and varying the number of pixels from 10 to 10 million. We then calculated the root mean squared error (RMSE) for each example, assuming that the probabilities from the high-resolution example approached those described by Equation 8. Figure 9 shows how the RMSE varies from pixel resolution when compared to the high-resolution example. We found that differences in detection probabilities decreased below 1% for all release radii when the number of pixels exceeded 5000; thus, we recommend pixel resolutions greater than 5000. Reducing potential uncertainties further by increasing pixel resolution will come at the cost of much higher computational effort, and may not be justified. Moreover, computational errors due to roundoff and approximations of probability functions become more critical.

Discussion

Determining the probability that a sampler array will intercept an elliptical release has been demonstrated for a variety of hypothetical examples. The results are dependent on the sampler locations, the radius of the release, and the aspect (eccentricity) and direction of the ellipse. Results are included for irregular sampling patterns in a finite size field for both uniform and nonuniform release probability density functions $p_s(x,y)$. Previous methods (e.g., Gilbert 1987 and Davidson 1995a, 1995b) considered only infinitely large fields, a uniform release probability across the field, and regular sampler patterns.

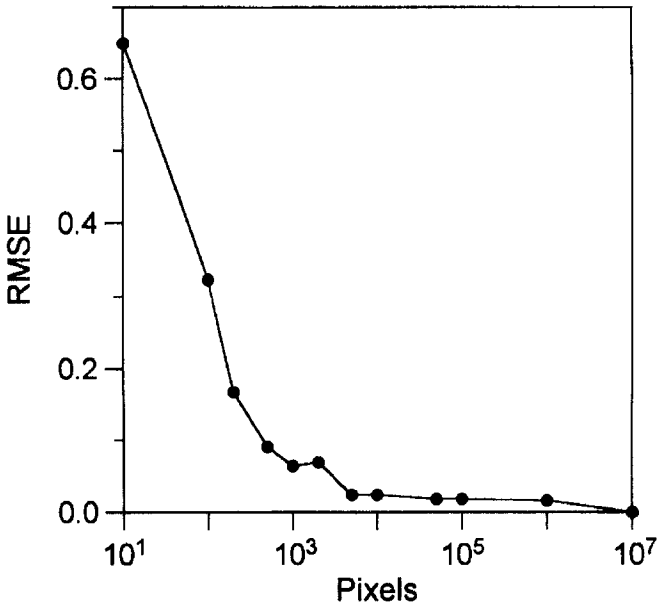

Figure 9. Root mean squared error (RMSE) associated with reducing pixel resolution. We assume that 10 million pixels approaches Equation 8, and the true probability.

For a regular pattern of samplers, the effect of the release probability density was somewhat minor for most of the calculations shown. This was true both for circular and elliptical releases with aspects of 0.5 (defined as ratio of minor to major axes), independent of the direction of ellipse orientation. However, when the sampler points were concentrated in the high release probability region, then the probability of a hit increased well above the uniform sampler pattern. This is shown in Figure 7. The effect will be more pronounced for more extreme release probability functions (i.e., releases with very high probabilities in localized regions, with near-zero values otherwise).

Optimal sampling patterns can be developed to account for a priori information about the field size, i.e., known subareas in the field where releases were more likely to have occurred. The approach suggests assigning new sampler locations or augmenting existing sampler locations taking into account more of the known historical information.

As discussed, the areal extent of measurement sensitivity of a sampler may be taken into account by extending the radius of the release ellipse by an effective radius of the sampler. Another more difficult problem deals with the fact that sensors offer varying degrees of reliability, so that the answer provided is not always a definite "yes" or "no." Sensor reliability may be addressed in part by extending the analysis to include probability of multiple hits. This would allow redundancy in the field monitoring system. Another approach is to simply retire one or more sensors from the calculations, which would simulate failures or ineffective measurements.

This analysis can, in principle, be codified and added as a module in saturated or unsaturated zone model packages. This could be done with only a small amount of extra data input. Then, as the model simulation progresses in time, and a contaminant plume develops in the flow field, the module would represent the plume as a binormal release function in the location predicted by the model. Multiple plumes generated by the model could be represented by multiple release functions. The module would then check proposed monitoring locations in relation to the release functions and determine the probability that the release intercepts a monitoring point. In this way, uncertainties in the detection algorithm are limited to uncertainties in the simulation itself. By treating certain model parameters (such as hydraulic conductivity) as random variables with known statistical properties, Monte Carlo flow and transport simulations can be performed to bracket conservative and nonconservative estimates of transport rates; hence, detection probabilities likewise would be bracketed and constrained by the same restrictions as the simulation model.

Acknowledgments

This research was supported by Western Regional Research Project W-188 and by the U.S. Nuclear Regulatory Commission (Contract #NRC-04-95-046).

References

Abramowitz, M., and I.A. Stegun (editors). 1964. Handbook of mathematical functions. Nat. Bureau Std. App. Math. Series, No. 55. Washington D.C.: U.S. Government Printing Office.

Davidson, J.R. 1995a. Elipgrid-PC: Upgraded version (ORNL/TM-13103). Oak Ridge, Tennessee: Oak Ridge National Laboratory.

Davidson, J.R. 1995b. Monte-Carlo tests of the Elipgrid-PC algorithm (ORNL/TM-12899). Oak Ridge, Tennessee: Oak Ridge National Laboratory.

Drew, L.J. 1967. Grid-drilling exploration and its application to the search for petroleum. *Economic Geology* 62, no. 5: 698-710.

Drew, L.J. 1979. Pattern drilling exploration: Optimum pattern types and hole spacings when searching for elliptical shaped targets. *Math. Geology* 11, no. 2: 223-253.

Freeze, R.A., J. Massmann, L. Smith, T. Sperling, and B. James. 1990. Hydrogeological decision analysis: 1. A framework. *Ground Water* 28, no. 5: 738-766.

Freeze, R.A., B. James, J. Massmann, T. Sperling, and L. Smith. 1992. Hydrogeological decision analysis: 4. The concept of data worth and its use in the development of site investigation strategies. *Ground Water* 30, no. 4: 574-588.

Gilbert, R.O. 1987. *Statistical Methods for Environmental Pollution Monitoring.* New York: Van Nostrand Reinhold Co.

Hammersley, J.M., and D.C. Handscomb. 1964. *Monte Carlo Methods.* New York: Metheun.

Keller, C. 1996. A reliable landfill monitoring system, leakage barrier, plus remediation method, in one design. Geol. Soc. Am. Abstracts with Programs 28, no. 1: 22. Boulder, Colorado: Geological Soc. America.

Loaiciga, H.A. 1989. An optimization approach for groundwater quality monitoring network design. *Water Resources Research* 25, no. 8: 1771-1782.

Meyer, P.D., A.J. Valocchi, and J.W. Eheart. 1994. Monitoring network design to provide initial detection of groundwater contamination. *Water Resources Research* 30, no. 9: 2647-2659.

Singer, D.A. 1972. ELIPGRID: A Fortran IV program for calculating the probability of success in locating elliptical targets with square, rectangular and hexagonal grids. *Geocom Programs* 4: 1-16.

Small, M.J. 1997. Groundwater detection monitoring using combined information from multiple constituents. *Water Resources Research* 33, no. 5: 957-969.

Young, M.H., P.J. Wierenga, A.W. Warrick, L.L. Hofmann, S.A. Musil, B.R. Scanlon, and T.J. Nicholson. 1996. Field testing plan for unsaturated zone monitoring and field studies. NUREG/CR-6462. Washington, D.C.: U.S. Nuclear Regulatory Commission.

Zirschky, J., and R.O. Gilbert. 1984. Detecting hot spots at hazardous-waste sites. *Chem. Engr.* 91, no. 14: 97-100.